Study on the in-elastic performance of mid-span gusset plate used in concentrically braced frames

P.C Ashwin Kumar, Afhaam Mannan, Anurag Anand & Dipti Ranjan Sahoo

Department of Civil Engineering, Indian Institute of Technology Delhi, India.

ABSTRACT: Detailed research work done over the years to optimize the performance of gusset plate has resulted in the evolution of an elliptical clearance limit for the corner gusset plate but relatively less amount of work has been done to improve the performance of the middle gusset plates. Currently, literature suggests to adopt a linear clearance limit of $6t_p$, where t_p is the thickness of the gusset plate but the experimental and analytical data supporting this notion is found lacking. So an attempt was made here using a continuum based software to understand the implications of adopting different varied linear clearances for mid span gusset plates. Two single storied frame models with two different brace slenderness (90 and 175), with four different linear clearances ($6t_p$, $8t_p$, $12t_p$ and $30t_p$) were developed and cyclic loads were applied to understand their response. It was found that if the middle gusset plate is properly designed then there is not much difference in the energy dissipation capacity of the frame and also the level of damage in the frame with lower slenderness ratio was found severe than the ones with higher slenderness ratio.

1 INTRODUCTION

Special concentrically braced frames (SCBFs) resist lateral forces induced by the ground motions effectively and economically. The preferred response of an SCBF system subjected to earthquake will be to dissipate this excess energy through the axial deformation of the braces but for this to happen, the response of the connection, which provides the pathway for the loads from the braces to the connecting members (beams and columns) is pivotal. The systems efficiency thus depends on the ability of the connections to tolerate large rotations such as those caused by the out-of-plane motion when the brace buckles. Additionally the connections must endure the compressive and tensile forces transferred by the brace during the cyclic deformation. Therefore, there should not be any untoward failure mechanism like buckling or connection fracture so as to render the brace to reach its full utility level. Over the years, many studies have been done to improve the performance of connections especially the design of gusset plates (Roeder et al., 2009). Providing a very large, stiff and strong gusset plate will limit the ductility of the brace whereas a small, weak and less stiff gusset may undergo premature fracture or failure. Thus, to render the brace to achieve its optimum, a balance needs to be maintained during the design and detailing of gusset plate. Past research works have already narrowed down the path for optimum gusset performance by studying on the various aspects of gusset plate performance. Requirements like the shape of gusset plate, clearance of the brace from the re-entrant corner, effect of edge stiffener plate and middle stiffener plate and the use of balanced design procedure for the design of gusset plates (Roeder et al., 2011) have been studied in detail. Least amount of study has been conducted to improve the performance of the middle gusset plate used in chevron and split-X type brace configuration. Where a corner gusset plate gets additional stiffness from the beam and column at its sides, the response of the middle gusset plate is entirely different as it has different boundary condition as well as it supports both tensile and compressive forces from the brace simultaneously.

2 MOTIVATION FOR STUDY

Extensive analytical and experimental investigations on the corner gusset plate has resulted in obtaining an elliptical clearance of 8tp, where tp is the thickness of the gusset plate, from the end of the brace to the re-entrant corner as shown in Fig.1a. This clearance level resulted in a compact gusset plate with adequate end rotation capabilities. Yoo (2008) performed a numerical investigation, where this 8tp elliptical clearance was used in the middle gusset plate model and its performance was compared to a 8tp linear clearance middle plate model, as shown in Fig.1b. The 8tp linear clearance model resulted in a smaller compact gusset plate and reduced the potential for premature gusset plate yielding. Another

analytical study (Hsiao, 2009) conducted on the middle gusset plate used linear clearance values of 2tp, 4tp, 6tp and 8tp for a single slenderness ratio of the brace. It was noticed from this study that by reducing the linear clearance limit, there was an increase in stress concentration within the middle gusset plate. Even though the 8tp model did not converge for drift value beyond 1.5%, credited to computational difficulty or excessive deformation in the model, the 6tp linear clearance model was suggested to be the optimum clearance for the middle gusset plate. The same was used in the experimental study and it performed well (Lumpkin et al 2012). This paper proceeds in the same path and explores the ideal clearance limit to provide more depth and clarity to previously done studies. Thus, braced frames having braces with two different slenderness ratio (90 and 175) and four linear clearance limit (6tp, 8tp, 12tp and 30tp) are used to understand the complex behavior of middle gusset plate. The corner gusset plate will follow the already established 8tp elliptical clearance for all simulation models.

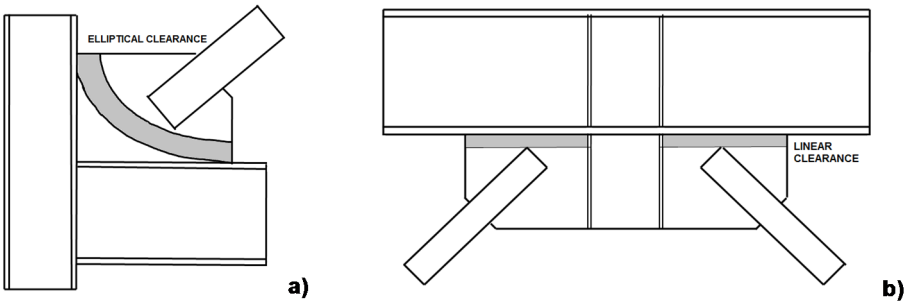

Fig. 1 – a) Elliptical Clearance in Corner Gusset Plate, b) Vertical Linear Clearance in Middle Gusset Plate

3 MODELING

To understand the inelastic response of the middle gusset plate subjected to cyclic loading, continuum finite element modeling of the frame has been done using a finite element software (ABAQUS, 2004). In the simulation study, four nodded shell elements with 6-degrees of freedom at each node with reduced-integration and large-strain formulation was used to model the braces, gusset plates, beams and columns. The frame with a bay width of 8m and height of 4m was modeled and gravity loads equivalent to an office building was assigned to the frame. Instead of designing the frame for a lateral force, the slenderness of the brace was selected, in this case 90 and 175, and the frame was designed for the maximum capacity of these braces along with the applied gravity load. The welding connections between the different members were not modelled explicitly. Instead, a rigid connection between them was assumed in the analysis. The meshing pattern consisted of a transition from the fine meshing to a coarser meshing in regions highly likely to undergo yielding. Fig.2 shows the mesh pattern adopted for the modelling of braced frame. Rigid (fixed) boundary conditions were imposed on the ends of both columns and the bottom of corner gusset plate. Two vertical stiffener plates has been provided on each side of the middle gusset plate to provide additional stiffness. The shape metrics was checked for each model considering the face corner angle and aspect ratio.

Since the design of beams and columns depends on the capacity of the braces, the sizes of beams and columns are different for both values of brace slenderness. Table 1 shows the sectional properties of the test frames for which the simulation model with four linear clearances namely, $6t_p$, $8t_p$, $12t_p$ and $30t_p$ each has been prepared. The balanced design procedure was adopted in designing the corner and middle gusset plate where, the procedure enhances the ductility of the brace by prioritizing the yield mechanism rather than failure. The corner gusset plate in all models has been designed by keeping an elliptical clearance of $8t_p$ whereas, the middle plate is modeled keeping the different vertical clearance limits.

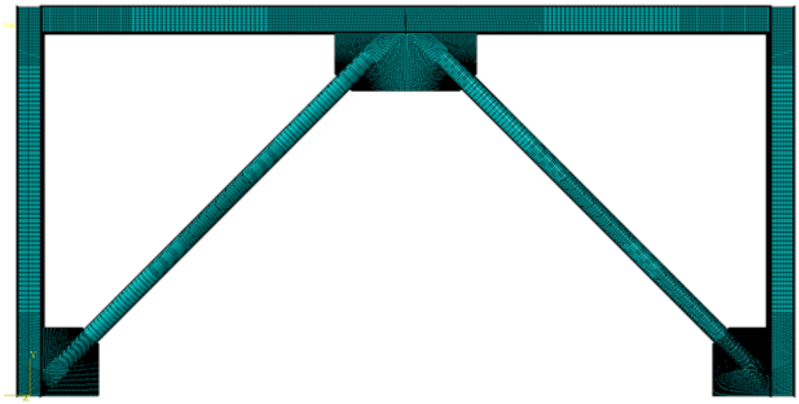

Fig. 2 – Mesh Pattern in the Simulation Model

Table 1 –Section specification of simulation model.

Brace Dia. mm	Brace Thick. mm	D/t	Slenderness Ratio	Gusset Plate Thick. mm	Beam	Column
164	8.85	18.53	**90**	10	W12X252	W12X252
90	4.85	18.56	**175**	8	W10X112	W10X112

4 MATERIAL PROPERTY FOR THE BRACES, GUSSET, BEAM AND COLUMNS

An isotropic hardening model implemented in ABAQUS to model the non-linear behavior of the material is not sufficient. It does not consider the cold working anisotropic effects that are introduced during cyclic loading. The reduction in the yield stress, which is known as the Bauschinger effect, is not, assimilated in isotropic hardening models. So to consider the effect of loading direction also, a combined isotropic and kinematic hardening rule has been assumed for this simulation study.

Since this study is mainly concentrated towards the simulation study, these parameters were taken from a previous research study on brace components (Fell, 2008). Table 2 gives the values of the nonlinear hardening parameter assumed for this study. Where, σ_y denotes the yield stress of the material; C and γ, collectively the kinematic hardening parameters, are the kinematic hardening moduli and the rate of decrease of kinematic hardening moduli with respect to increasing plastic deformations respectively. They both collectively contribute in the calculation of the overall back-stress developed. Q_∞ and b are the isotropic hardening parameters. Where, Q_∞ relates to the maximum change in the size of the yield surface and b relates to its rate of change as the plastic strain develops.

Table 2 – Calibrated kinematic and isotropic hardening law.

	σ_y N/mm^2	C N/mm^2	γ	Q_∞N/mm^2	b
Brace	380	3448	35	359	2
Gusset	345	3448	38	118	5
Beam	414	3448	35	391	2
Column	414	3448	35	391	2

A damage model was also included in the model to simulate low cycle fatigue fracture. A damage initiation parameter and a damage evolution parameter were defined to simulate the degradation of the material stiffness once the corresponding initiation criterion was reached. Of the two prominent mechanisms for fracture in ductile metals, which includes nucleation, growth, and coalescence of voids; and shear fracture due to shear band localization, the former was used in predicting the onset of damage in the members.

5 LOADING PROTOCOL

The standard cyclic loading protocol which has been adapted from ATC-24 (1992) guidelines and used in other experimental investigation (Fell 2008) has been used for this study. Since the response of the braced frame rely on the brace configuration as well as the buckling of the compression brace, the loading protocol has been modified to represent the braced frame as per the guidelines set by Krawinkler et al. (2000). As shown in the Fig.3, the loading protocol consists of three elastic steps comprising of six drift cycles each, followed by four cycles corresponding to the onset of inelasticity in the system. In this case, the onset of inelasticity was considered as the initiation of brace buckling under the compressive loading. In total 9 cyclic loading steps were applied with a maximum brace deformation in this study fixed corresponding to a story drift of 5% as recommended by (Sabelli et al.,2013).

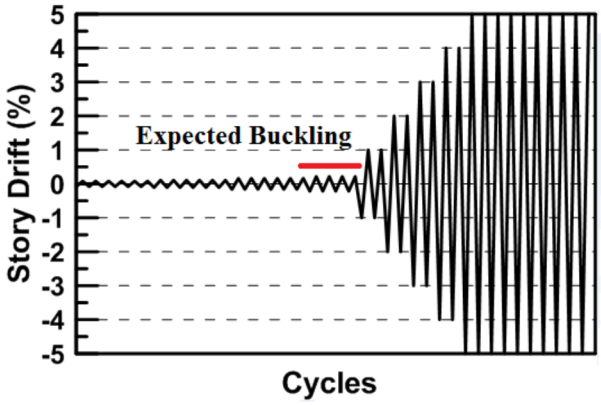

Fig. 3 – Standard cyclic loading protocol used in this study

6 RESULTS

6.1 Brace Slenderness 90

The simulation models with linear clearance of $6t_p$, $8t_p$ and $12t_p$ ran beyond 3% storey drift until it stopped either due to computational difficulty or due to large deformations occurring in the frame. The $30t_p$ model failed at an early stage due to the buckling and eventually tearing of the middle gusset plate as the thickness of 10mm of the plate did not satisfy the buckling strength requirement using the Thornton method. The state of the middle gusset plate in the $30t_p$ model is as shown in Fig.4a.

If the results are interpreted until the point where the simulation has run then, the hysteresis plot of the base shear versus lateral displacement, Fig.5a, and the cumulative energy versus drift, Fig.5b, for all the linear clearance model shows the trend that there is not much difference in the response of these models. If the instances of initiation of gusset fracture is compared as in Table 3, it is seen that as the linear clearance limit is increased there is a delay in the initiation of fracture in the gusset plate. Fig.4b shows the location of these fracture initiation points and Fig.6a and b shows the state of the corner and middle gusset plate under the applied lateral deformations. It can also be seen that the corner gusset plate as well as the middle gusset plate develop the elliptical yielding pattern, which reinforces the experimental and analytical findings published earlier. It is also seen from the table that there is an initiation of junction tear in the corner gusset plate indicated at location “JT” in Fig.4b and this failure was specific to this lower slenderness ratio. As the lateral deformations were applied to the left end of the frame, the degree of damage was more seen at the left corner gusset plate. The damage in the gusset although did not result in complete failure of the gusset plate but excessive damage or element deletion was seen in the brace slenderness 90 group than in brace slenderness 175 group.

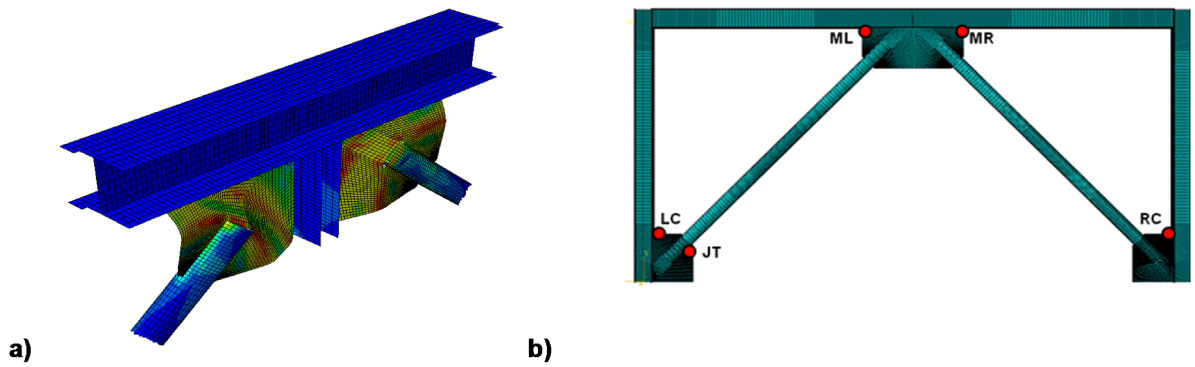

Fig. 4 – a) Buckling of middle gusset plate for 30tp linear clearance model, b) Locations of initiation of tear in gusset plate

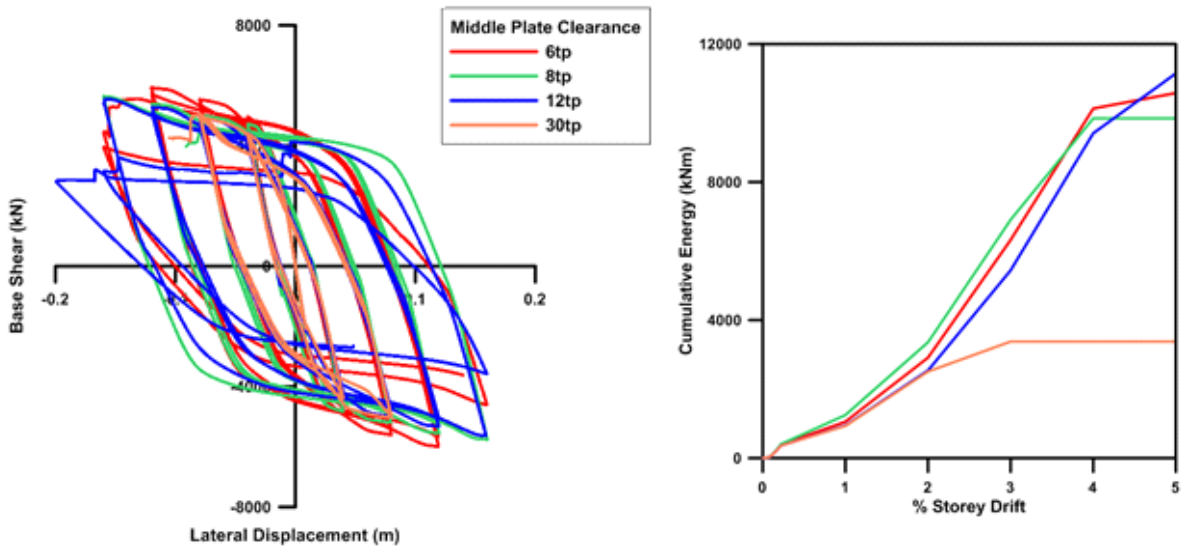

a) b)

Fig. 5 – a) Hysteresis Curves for Linear Clearance Models, b) Cumulative Energy Dissipated for Linear Clearance Models

Table 3 – Instances of initiation of tear in gusset plate.

Initiation of Tearing	**$6t_p$**	**$8t_p$**	**$12t_p$**
Left Corner Gusset (LC)	Start of 2%	Start of 2%	Start of 2%
Right Corner Gusset (RC)	Start of 2%	Start of 3%	End of 2%
Middle Plate Right-end (MR)	End of 2%	End of 3%	Start of 5%
Middle Plate Left-end (ML)	Start of 3%	End of 3%	End of 4%
Brace Gusset Junction Tear (JT)	Middle of 3%	End of 3%	Start of 4%
Simulation Ended	Middle of 4%	Middle of 4%	Start of 5%

Base Shear Contribution

Fig.7 shows the contribution of different members of the frame in resisting the lateral deformations for different linear clearance of middle gusset plate. Where, column 1 represents the reaction in the column on the left end of the frame, at which end the lateral deformation is applied. It is quite evident from the figure that the left side column is taking the majority of the base shear. In the part of the load cycle

where the brace has not buckled under compression it takes the majority of the base shear component but as the braces buckle its base shear contribution decreases.

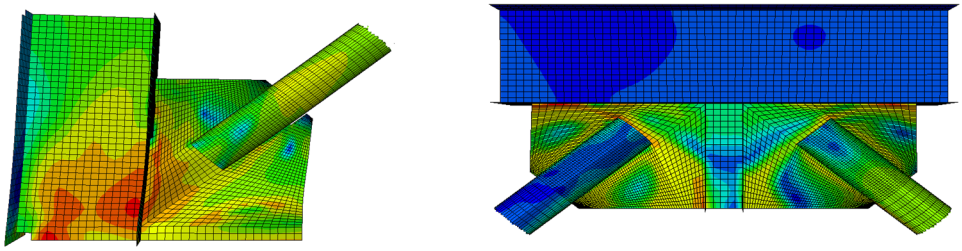

a) b)

Fig. 6 – a) State of corner gusset plate, b) State of middle gusset plate

Near the 1.5% drift mark for linear clearance model of $6t_p$, $8t_p$ and $12t_p$ it dips below the right column contribution levels. To provide uniformity to the results, results up to 3% lateral has been shown in the figure. The 6tp linear clearance model shows more degradation in the brace contribution than the 8tp or $12t_p$ model, this may be attributed to the increased rotational stiffness of the 6tp middle plate. The 30tp linear clearance model shows a varied response, as its brace contribution was higher than other models. Although as discussed earlier this model failed due to the middle gusset plate buckling, the contribution of the tension brace and almost zero effect of the compression brace might have caused this increase.

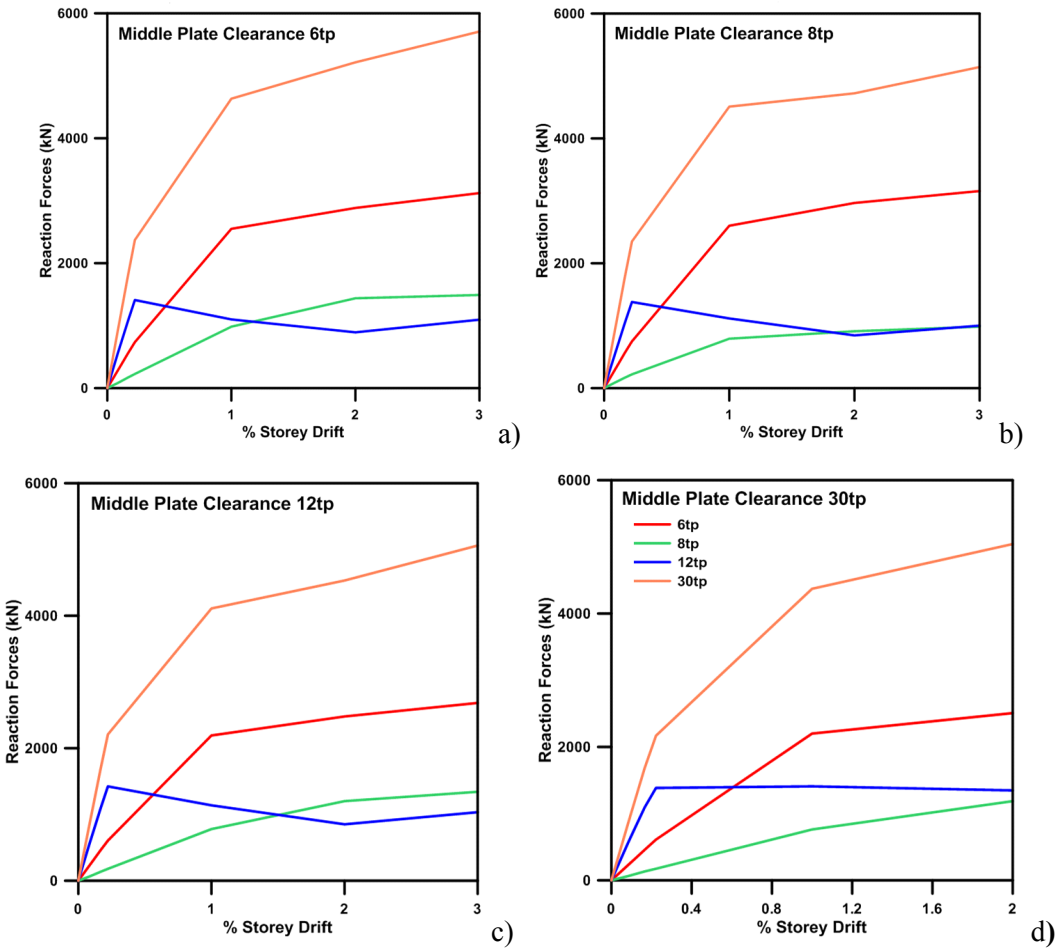

Fig. 7 – Base shear contribution of columns and braces for varying linear clearance model

6.2 Brace Slenderness 175

The simulation models with linear clearance of $6t_p$, $8t_p$, $12t_p$ and $30t_p$ ran beyond 4% storey drift until it stopped due to reasons mentioned above. Unlike the brace slenderness ratio 90 models the gusset plate

thickness selected for this group satisfied the buckling strength criteria, even for the 30tp linear clearance model. Similar to the previous group, if the results are interpreted till the point where the simulation has run then, the hysteresis plot of the base shear versus lateral displacement, Fig.8a, and the cumulative energy versus drift, Fig.8b, for all the linear clearance model again shows similar trend that there is not much difference in the response of these models. The 30tp linear clearance model is showing a peak in Fig. 9b as the results include the effect till the end of the 5% drift and only the 30tp model ran the complete lateral deformation cycle.

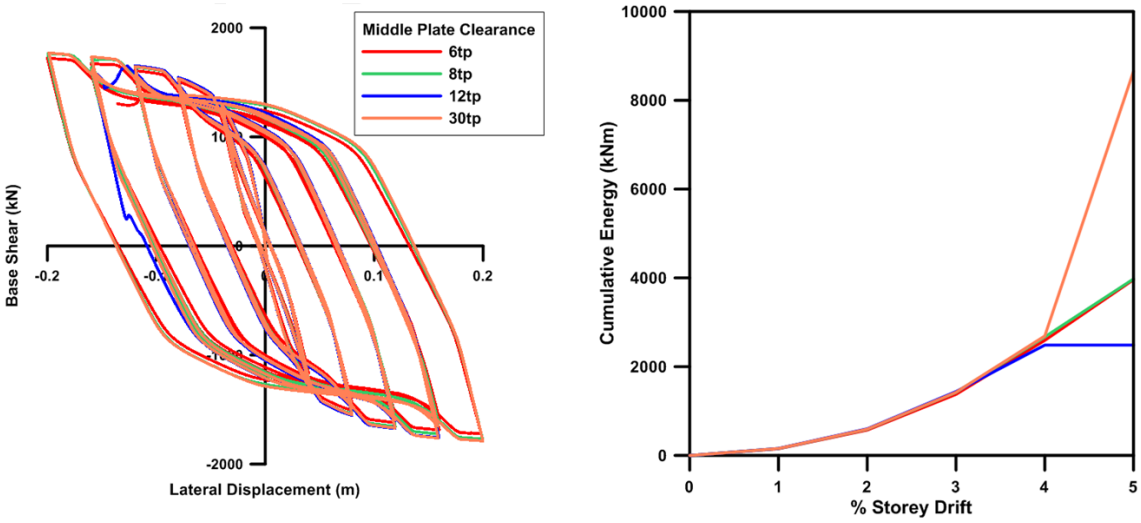

a) b)

Fig. 8 – a) Hysteresis curves for linear clearance models, b) Cumulative energy dissipated for linear clearance models

Table 4 – Instances of initiation of tear in gusset plate.

Initiation of Tearing	**$6t_p$**	**$8t_p$**	**$12t_p$**	**$30t_p$**
Left Corner Gusset (LC)	Start of 3%	Start of 3%	Start of 3%	Start of 3%
Right Corner Gusset (RC)	End of 3%	End of 3%	End of 3%	End of 3%
Middle Plate Left-end (MR)	Middle of 4%	Absent	Absent	Absent
Middle Plate Right-end (ML)	End of 4%	Absent	Absent	Absent
Brace Gusset Junction Tear (JT)	Absent	Absent	Absent	Absent
Simulation Ended	Start of 5%	Start of 5%	Start of 5%	End of 5%

If the instances of initiation of gusset fracture is compared as in Table 4, it is again seen that as the linear clearance limit is increased there is a delay in the initiation of fracture in the gusset plate. For the $8t_p$, $12t_p$ and $30t_p$ model there is no tear in the middle gusset plate and there is no junction tear as seen earlier. This in a way indicates that by using braces of higher slenderness ratio there is less damage to the gusset plate and the chances that the brace achieves its optimum performance level is also increased. On the downside of this notion it must be kept in mind that braces with higher slenderness ratio can resist lower magnitudes of tensile and compressive forces.

Base Shear Contribution

The contribution of different members of the frame in resisting the lateral deformations for different linear clearance of middle gusset plate. The results in the brace slenderness ratio 175 also showed similar trend as the slenderness ratio 90 group. In the part of the load cycle where the brace has not buckled under compression it takes the majority of the base shear component but as the braces buckle its base shear contribution decreases. and $30t_p$ it dips below the right column contribution levels.

7 CONCLUSION

Through this simulation study, which was directed at understanding the response of middle gusset plate, the following conclusions can be drawn from it:

- For brace slenderness of 90 and 175, with gusset plates (middle or corner) designed using the balanced design approach, the linear clearance models showed no major variation in energy dissipation capabilities.
- Frames with brace slenderness 90 was more prone to damage in gusset plates than frames with higher brace slenderness of 175.
- Junction tear and tear initiation in the middle gusset plate occurred for frames with brace slenderness 90 whereas these two damage states was totally absent for frames with brace slenderness of 175 except for the 6tp model but there too it was not as severe as its counterparts.
- Frames with braces of higher slenderness showed delayed instances of initiation of tear in gusset plates compared to the ones with lower slenderness. Thus, supporting the notion to use braces with higher slenderness ratio to resist lateral loads.
- For both slenderness ratio groups it was commonly seen that as the linear clearance of the middle plate was increased there was reduction in the stress concentration and thus reduced tearing in the plates was noticed.
- The contribution of the brace in sharing the lateral force was the maximum before the onset of inelasticity in the system. Once the brace buckled the columns took over the mantle to resist these forces. It was seen in general that the resistance share of the brace fell below both columns in between the 1.5% to 2 % lateral drift levels.
- It was noticed that there was a reduction in the brace strength contribution for the middle plate if it is subjected to tensile and compressive forces simultaneously, which is the general loading condition. This needs to be probed further as improvement in the stiffness of the middle gusset plate may help to increase the brace's energy dissipation capacity.

REFERENCES:

ABAQUS. 2004. *ABAQUS User's Manual*, *Version 6.10.* Hibbit, Karlsson, and Sorenson, Inc. Providence, RI.

ATC-24. 1992. Guidelines for cyclic seismic testing of components of steel structures for buildings. *Report No. ATC-24.* Applied Technology Council. Redwood City, CA.

Fell B.V. 2008. Large-scale testing and simulation of earthquake-induced ultra-low cycle fatigue in bracing members subjected to cyclic inelastic buckling. *Doctoral thesis*. University of California at Davis, CA.

Hsiao P.C. 2009. Simulation Methods for Special Concentrically Braced Frames. General Examination, Department of Civil Engineering. University of Washington, Seattle. December.

Krawinkler H.K., Gupta A, Median R.A., Luco N. 2000. Loading histories for seismic performance testing of SMRF components and assemblies. *Report No. SAC/BD-00/10*. SAC Joint Venture. Sacramento, CA.

Lumpkin E.J., Hsiao P.C., Roeder C.W., Lehman D.E., Tsai C.Y., Wu A.C., Wei C.Y., Tsai K.C. 2012. Investigation of the seismic response of three-story special concentrically braced frames. *Journal of Constructional Steel Research*. 77(10). 131-144.

Roeder C.W., Lehman D.E., Lumpkin E.J. & Hsiao, P.-C. 2009. Seismic Evaluation and Rehabilitation of Concentrically Braced Frames. In *ATC & SEI 2009 Conference on Improving the Seismic Performance of Existing Buildings and Other Structures*. 777–788.

Roeder C.W., Lumpkin E.J., Lehman D.E. 2011. A balanced design procedure for special concentrically braced frame connections. *Journal of Constructional Steel Research.* 67(11). 1760-1772.

Sabelli R, Roeder C.W., Hajjar J.F. 2013. Seismic design of steel special concentrically braced frame systems: A guide for practicing engineers. *NEHRP Seismic Design Technical Brief No. 8.* Gaithersburg, MD.

Yoo J.H. 2008. Simulated Behavior of Multi-Story X-Braced Frames. *Engineering Structures*. 182-197.